A 17.3 GHZ ATOMIC-LAYERED HZO SOLIDLY MOUNTED RESONATOR: TOWARDS CMOS-BEOL MM-WAVE FREQUENCY CONTROL

*T. Tharpe**, *S. Dabas, D. Mo, and R. Tabrizian*

Electrical and Computer Engineering Department, University of Florida, Gainesville, Florida, USA

ABSTRACT

This paper reports, for the first time, on a 17.3 GHz hafnia-zirconia (HZO) solidly mounted bulk acoustic wave (BAW) resonator created entirely by atomic layer deposition. CMOS-based ferroelectric, dielectric, and metallic layers with atomically precise thicknesses are stacked to realize a solid-state acoustic cavity with ultra-uniform frequency across the wafer and for back-end-of-line (CMOS-BEOL) integration. The resonator prototype demonstrates a large electromechanical coupling (k_t^2) of 3.62% and a high-quality factor (Q) of 267, setting a new $k_t^2.Q$ record of ~10 at such high operation frequency. Intrinsic switchability is also demonstrated for the resonator, based on exploiting ferroelectric polarization tuning in HZO.

KEYWORDS

Super-high-frequency, CMOS BEOL, solidly mounted resonator, ferroelectric, hafnia-zirconia, intrinsically switchable.

INTRODUCTION

Since demonstration of the resonant gate transistor by Nathanson et. al. in the 1960s [1], monolithic integration of mechanical / acoustic resonators on semiconductor platforms has been vigorously followed. This is primarily driven by the overhead of non-monolithic integration approaches that set fundamental limits on the performance, footprint, and cost of microsystems relying on frequency generation and control.

Having access to high Q and k_t^2 acoustic resonators on standard semiconductor nodes can potentially revolutionize data processing and wireless communication systems by accommodating high-performance local oscillators, clocks, and spectral processors in ultra-miniaturized footprints. Successful demonstrations of CMOS-monolithic resonators include innovative approaches relying on front-end-of-line (FEOL) building blocks (*e.g.*, FinFET) [2] or BEOL metal and dielectric layers [3] to create high-Q resonators. These approaches generally rely on electrostatic transduction, which substantially limit their k_t^2 and make extreme frequency scaling to cm- / mm-wave challenging.

The observation of ferroelectric behavior in hafnia-zirconia ($Hf_{0.5}Zr_{0.5}O_2$ or HZO), and the first demonstration of HZO nano-electro-mechanical transducers [4] have augured the potential for realization of long-coveted CMOS-monolithic high $k_t^2.Q$ acoustic resonators. HZO films, commonly used in amorphous form as high-k dielectric material of advanced CMOS, can be crystallized upon proper application of stress. HZO films deposited by ALD, and stress-engineered by capping electrodes, provide a large remanent polarization and piezoelectric coupling, even upon scaling to sub-5nm. However, the major challenge in using HZO for creation of high $k_t^2.Q$ resonators is the large dependence of its polarization and piezoelectricity on residual stress (also called crystallization stress). As recently demonstrated [5], releasing HZO transducers to create free-standing resonators results in significant degradation of their polarization and piezoelectricity.

In this work, for the first time we demonstrate a solidly mounted resonator (SMR) based on integration of HZO transducer on Bragg acoustic reflectors created from alternating ALD of tungsten (W) and silicon dioxide (SiO_2). This architecture sustains the crystallization-stress, large polarization, and piezoelectricity in

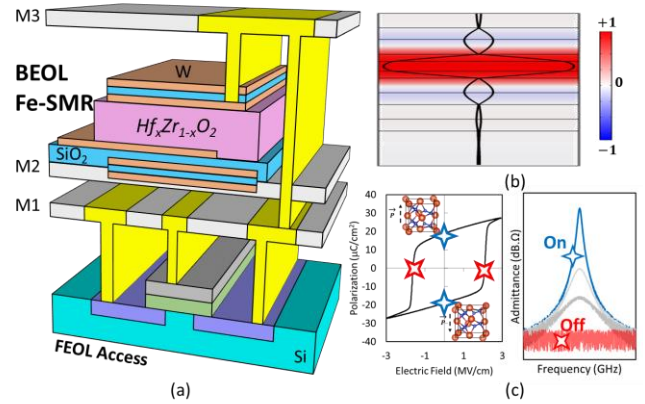

Fig. 1: *(a) Conceptual schematic of atomic-layered HZO SMR integrated on CMOS-BEOL. (b) COMSOL-simulated resonator mode-shape, showing the thickness-extensional stress across the stack. (c) Ferroelectric HZO polarization hysteresis loop and resonator frequency response, highlighting intrinsic switchability.*

HZO facilitating creation of high k_t^2 BAW resonators. Further, the all-ALD fabrication process enables extreme frequency scaling to mm-wave, while benefiting from frequency definition with ultra-high precision, only limited by atomic-level thickness of constituent layers. The CMOS-based materials and processing, and solid-state architecture of the presented resonator makes it perfectly compatible for CMOS-BEOL integration (Fig. 1).

CONCEPT

Figure 1 conceptually shows the atomic-layered HZO SMR created by stacking HZO transducer within W/SiO_2 Bragg reflectors. The reflectors not only localize acoustic energy for high-Q operation, but also sustain the crystallization-stress in HZO required for large piezoelectric coupling. Figure 1(b) shows the COMSOL-simulated stress-profile across the resonator stack, highlighting the thickness-mode localization in HZO transducer. Figure 1(c) shows the polarization-hysteresis loop for ferroelectric HZO transducer and conceptual resonator admittance response, highlighting the capability of intrinsic switching by DC-tuning of polarization. This feature is highly desirable for creation of multi-frequency oscillators and multi-band configurable filters.

HAFNIA-ZIRCONIA TRANSDUCER

Transduction of thickness-mode BAW in HZO resonators is achieved via the piezoelectric effect inherent to all ferroelectrics. Upon application of sufficient crystallization stress and limitation of grain size, the polar orthorhombic phase (space group $Pca2_1$) is stabilized. However, due to HZO's inherent polymorphism and acute dependence on residual stress, nonpolar tetragonal and monoclinic phases readily form in the presence of stress nonuniformities. Figure 2 depicts the effect of stress boundary condition on the ferroelectric performance, and therefore orthorhombic composition, of an HZO transducer. Figure 2 (a) shows polarization vs electric field hysteresis measurements for fabricated HZO SMR prototypes, highlighting how a solidly mounted architecture results in a higher remanent polarization and

less paraelectric loop slanting, indicative of higher orthorhombic percentage. Figure 2 (b) shows how the higher ferroelectric phase contribution in solidly mounted architectures results in increased displacement vs electric field (*i.e.*, piezoelectric coupling).

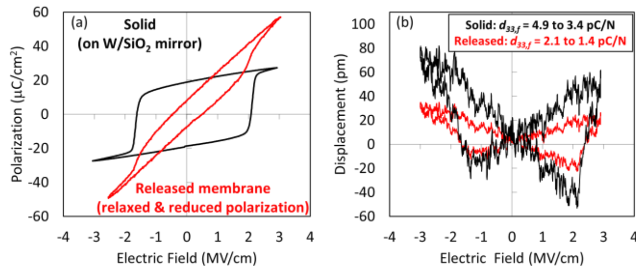

Fig. 2: *(a) Polarization vs electric field and (b) displacement vs electric field hysteresis for solidly mounted W-HZO-W capacitors and released membranes.*

RESONATOR FABRICATION

HZO SMR is fabricated using the process depicted in Fig. 3. First, an acoustic Bragg mirror is formed via four, alternating depositions of 65.5nm ALD W and 81.5nm of ALD SiO_2. Next, 34nm W is ALD and patterned for device bottom electrodes, followed by deposition and patterning of platinum (Pt) routing. The ~50nm thick device transducer, composed of 5, 9nm ALD HZO layers intercalated with 4, 1nm ALD alumina (Al_2O_3) layers is then capped with a symmetric 34nm top W electrode and rapid thermal annealed at 500ºC for 20s in nitrogen ambient. Top electrodes are patterned, and access windows to bottom W electrodes etched, respectively using reactive ion etching. Finally, top Pt is sputtered and lifted off for pads and routing.

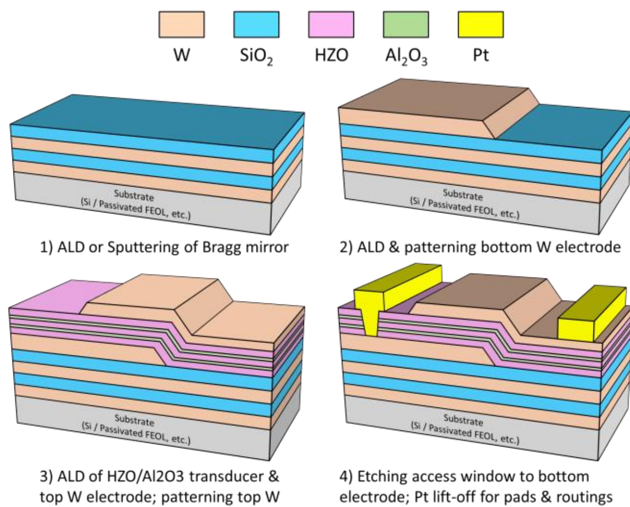

Fig. 3: *Four-step fabrication process for creation of CMOS-BEOL compatible, high k_t^2.Q, HZO transduced, SMR resonators.*

Optical images of the finalized HZO resonator are shown in Fig. 4 (a). Figure 4 (b) depicts a scanning electron microscope (SEM) image of the device active area, highlighting the ~8μm x ~8μm W top electrode used to mitigate lateral wave propagation. Figure 4 (c) shows a cross-sectional SEM image of the HZO nanolaminate transducer atop alternating Bragg-mirror layers. Insets depict a cross sectional transmission electron microscope (XTEM) image of interposed transducer layers with annotated thicknesses and a high-angular dark-field (HAADF) STEM of an orthorhombic grain with measured ~34º c-axis orientation.

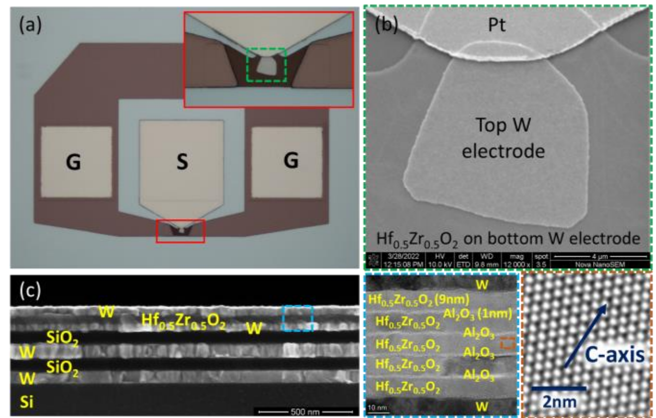

Fig. 4: *(a) Optical image of fabricated HZO SMR BAW resonator. (b) SEM image highlighting device active area. (c) Cross-sectional SEM with constituent layers annotated and inset XTEM of the HZO nanolaminate transducer with further inset depicting HAADF STEM of individual orthorhombic grain.*

RESONATOR CHARACTERIZATION

Figure 5 (a) depicts measured admittance ($|Y_{11}|$) for the HZO SMR at different bias voltages applied using bias-tee. A k_t^2 of 3.62% and Q of 267 is measured at 17.3 GHz. Figure 5 (b) shows the switching trend of admittance as voltages near coercive.

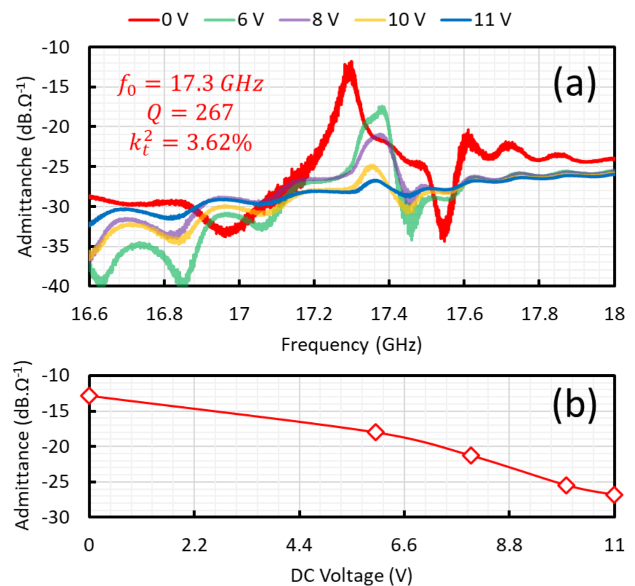

Fig. 5: *(a) Admittance responses for an ~8μm x ~8μm HZO SMR BAW resonator, colored by DC bias voltage. (b) Extracted switching trend of admittance at voltages nearing coercive.*

ACKNOWLEDGEMENTS

This work is supported under the DARPA YFA program.

REFERENCES

[1] H. C. Nathanson, et. al., IEEE TED, vol. 14, no. 3, p. 117.
[2] B. Bahr, et. al., IEEE ISSCC 2018.
[3] M. Li, et. al., IEEE JMEMS, vol. 24, no. 2, p. 360.
[4] M. Ghatge, et. al., IEEE IEDM 2018.
[5] T. Tharpe, et. al., Adv. Eng. Mat, vol. 23, no. 12, 2021.

CONTACT

*T. Tharpe, tel: +1-321-432-9557; ttharpe@ufl.edu